Title
Real-time phase-resolved optical coherence tomography and optical Doppler tomography

Journal
Optics Express, 10(5)

ISSN
1094-4087

Authors
Ding, Zhihua
Zhao, Yonghua
Ren, Hongwu
et al.

Publication Date
2002-03-11

DOI
10.1364/OE.10.000236

Peer reviewed

Real-time phase-resolved optical coherence tomography and optical Doppler tomography

Zhihua Ding, Yonghua Zhao, Hongwu Ren, J. Stuart Nelson, and Zhongping Chen

Beckman Laser Institute and Center for Biomedical Engineering
University of California, Irvine, CA 92612

zchen@bli.uci.edu, zhding@laser.bli.uci.edu

Abstract: We have developed a novel real-time phase-resolved optical coherence tomography (OCT) and optical Doppler tomography (ODT) system using optical Hilbert transformation. By combining circularly polarized reference and linearly polarized sample signals, in-phase and quadrature interference components are produced in separate channels and treated as the real and imaginary parts of a complex signal to obtain the phase information directly. Using a resonant scanner at an axial scanning speed of 4 kHz in the reference arm of the interferometer, both structure and blood flow velocity images with 200 axial scans can be acquired at 20 frames per second with high sensitivity and large dynamic range. Real-time videos of *in vivo* blood flow in the chick chorioallantoic membrane using this interferometer are presented.

OCIS codes: (170.1650) Coherence imaging; (100.6950) Tomographic image processing

References

1. D. Huang, E. A. Swanson, C. P. Lin, J. S. Schuman, W. G. Stinson, W. Chang, M. R. Hee, T. Flotte, K. Gregory, C. A. Puliafito, and J. G. Fujimoto, "Optical coherence tomography," Science **254**, 1178-1181 (1991).
2. Z. Chen, T. E. Milner, D. Dave, and J. S. Nelson, "Optical Doppler tomographic imaging of fluid flow velocity in highly scattering media," Opt. Lett. **22**, 64-66 (1997).
3. Z. Chen, T. E. Milner, S. Srinivas, X. J. Wang, A. Malekafzali, M. J. C. van Gemert, and J. S. Nelson, "Noninvasive imaging of *in vivo* blood flow velocity using optical Doppler tomography," Opt. Lett. **22**, 1119-1121 (1997).
4. J. A. Izatt, M. D. Kulkarni, S. Yazdanfar, J. K. Barton, and A. J. Welch, " *In vivo* bidirectional color Doppler flow imaging of picoliter blood volumes using optical coherence tomography," Opt. Lett. **22**, 1439-1441 (1997).
5. Z. Chen, T. E. Milner, X. J. Wang, S. Srinivas, and J. S. Nelson, "Optical Doppler tomography: Imaging *in vivo* blood dynamics following pharmacological intervention and photodynamic therapy," Photochem. Photobiol. **67**, 56-60 (1998).
6. Y. Zhao, Z. Chen, C. Saxer, S. Xiang, J. F. de Boer, and J. S. Nelson, " Phase-resolved optical coherence tomography and optical Doppler tomography for imaging blood flow in human skin with fast scanning speed and high velocity sensitivity," Opt. Lett. **25**, 114-116 (2000).
7. Z. Chen, Y. Zhao, S. M. Srinivas, J. S. Nelson, N. Prakash, and R. D. Frostig, "Optical Doppler tomography," IEEE J. of Selected Topics in Quantum Electronics **5**, 1134-1141 (1999).
8. U. Morgner, W. Drexler, X. D. Kartner, C. Piltris, E. P. Ippen, and J. G. Fujimoto, "Spectroscopic optical coherence tomography," Opt. Lett. **25**, 111-113 (2000).
9. C. E. Saxer, J. F. de Boer, B. H. Park, Y. Zhao, Z. Chen, and J. S. Nelson, " High-speed fiber based polarization-sensitive optical coherence tomography of *in vivo* human skin," Opt. Lett. **25**, 1355-1357 (2000).
10. Y. Zhao, Z. Chen, C. Saxer, Q. Shen, S. Xiang, J. F. de Boer, and J. S. Nelson, " Doppler standard deviation imaging for clinical monitoring of *in vivo* human skin blood flow," Opt. Lett. **25**, 1358-1360 (2000).
11. Y. Zhao, Z. Chen, Z. Ding, H. Ren, J. S. Nelson, "Real-time phase-resolved functional optical coherence tomography by use of optical Hilbert transformation," Opt. Lett. **27**, 98-100 (2002).

#726 - $15.00 US Received January 18, 2002; Revised February 26, 2002

12. C. Yang, A. Wax, R. R. Dasari, and M. S. Feld, "Phase-dispersion optical tomography," Opt. Lett. **26**, 686-688 (2001).
13. M. Sticker, C. K. Hitzenberger, R. Leitgeb, and A. F. Fercher, "Quantitative differential phase measurement and imaging in transparent and turbid media by optical coherence tomography," Opt. Lett. **26**, 518-520 (2001).
14. A. M. Rollins, S. Yazdanfar, J. K. Barton, J. A. Izatt, "Real-time *in vivo* color Doppler optical coherence tomography," J. Biomed. Opt. **7**, 123-129 (2002).

1. Introduction

Optical coherence tomography (OCT) [1] is a noninvasive, noncontact imaging modality that uses coherent gating to obtain high-resolution cross-sectional imaging of tissue microstructure. OCT is analogous to ultrasound imaging except that infrared light waves rather than acoustic waves are used. Consequently, the spatial resolution of OCT is more than an order of magnitude better than that of the ultrasound imaging. Several extensions of OCT have been developed for functional imaging of tissue physiology. Optical Doppler tomography (ODT), for example, combines Doppler principle with coherence gating for tomographic imaging of tissue structure and blood flow, simultaneously [2-7]. Spectroscopic OCT combines spectroscopic analysis with OCT to obtain depth resolved tissue absorption spectra [8]. Polarization sensitive OCT (PS-OCT) combines polarization sensitive detection with OCT to determine tissue birefringence [9].

Given the noninvasive nature and exceptional high spatial resolution (2-10 μm), ODT has a number of potentially important clinical applications. Examples include evaluating the efficiency of laser treatment of port wine stains and photodynamic therapy, screening vasoactive and antiangiogenic drugs, skin cancer diagnosis, and monitoring cortical activity and brain injury. In order to be useful for *in situ* diagnostics, ODT must provide clinicians with real-time imaging.

ODT is based on the principle that light interacting with moving particles, such as red blood cells (RBCs) inside biological tissues, cause Doppler frequency shifts in the measured interference signal. One straightforward way to detect Doppler frequency shifts is the spectrogram method based on the fast Fourier transform (FFT) algorithm [2-4]. Since detection of the Doppler frequency shift requires sampling the interference signal over at least one oscillation cycle, the minimum detectable Doppler frequency shift varies inversely with the FFT window time at each pixel, which introduces a tradeoff between velocity sensitivity and imaging speed as well as spatial resolution. We previously reported a phase-resolved method [6,7,10] that can decouple the velocity sensitivity from the spatial resolution while maintaining a high acquisition speed. The phase is determined by the complex-valued analytic function derived from an analytic continuation of the measured interference signal. Phase-resolved OCT/ODT [6,7,10,11] uses the phase change between the measured interference signals from sequential axial scans for velocity image reconstruction. Because the time interval between sequential axial scans is much longer than the FFT window time at each pixel, velocity sensitivity is greatly improved when compared to the spectrogram method [6,7,10]. In addition to velocity imaging, the phase-resolved method has also been adapted to image and quantify other physiological parameters such as birefringence, dispersion, and spatial phase variations [9,12,13]. However, the maximum determinable Doppler frequency shift using the phase-resolved method is limited by the Nyquist sampling theorem to half of the axial scanning frequency. Current systems utilizing a rapid scanning optical delay line (RSOD) can only measure a maximum Doppler frequency shift of 500 Hz when a nonresonant galvanometer operates at its highest scanning frequency of 1 kHz. Replacing the current galvanometer with a resonant scanner at a scanning frequency of 4-8 kHz greatly increases the maximum determinable Doppler frequency shift. However, fast scanning leads to other problems. First, for implementation of the phase-resolved method with high accuracy [6,7,10], phase modulation is required to generate a sufficiently large carrier frequency in the interference signal so that there are at least two fringes per coherence

#726 - $15.00 US Received January 18, 2002; Revised February 26, 2002

length scanned. Accordingly, the phase modulation frequency needs to be increased proportional to the axial scanning frequency. Higher carrier frequency in the interference signal requires a broader bandwidth of the photo-amplifier for detection. Designing a circuit with low noise and broad bandwidth is challenging. Second, higher carrier frequency in the interference signal requires a higher data acquisition rate, which complicates the system design. Third, a higher data acquisition rate requires a faster data processing speed for reconstruction of the image in real-time. There are two possible solutions for these limitations. One approach utilizes a custom-designed digital signal processor (DSP) to accelerate the post-detection computation; the other implements a real-time detection technique based on custom-designed hardware to reduce the post-detection computational overhead [11,14].

In this paper, we describe in detail a technique to overcome the aforementioned limitations by incorporating an optical Hilbert transformation into our phase-resolved OCT/ODT system. This approach combines circularly polarized reference and linearly polarized sample signals, which introduces a 90 degree phase shift in the interference signal. The real and imaginary parts of the interference field are produced in two output channels based on polarization discrimination. This method generates analytical continuation optically and does not have the restriction on phase modulation frequency. Using a high-speed RSOD based on a resonant scanner in combination with the proposed optical Hilbert transformation technique, real-time simultaneous images of tissue structure and blood flow velocity can be obtained.

2. Theory

We previously described the tradeoff between imaging speed and velocity sensitivity. High frame rate as well as high velocity sensitivity can be achieved by the phase-resolved OCT/ODT technique [6,7,10]. Moving particles within the sample can cause phase changes in the interference signal. By comparing the phase change of the same pixel between sequential scans, velocity information can be obtained with high sensitivity while maintaining high spatial resolution. The key to this technique is the use of phase information from the interference signal.

2.1 Post-detection digital approach for phase-resolved OCT/ODT

In this section, we describe the basic concept behind the post-detection digital approach for obtaining the phase-resolved analytic signal from the real interference signal. Considering a time-varying interference signal $\Gamma(t)$, one way to represent this is by an integral of elementary complex exponential functions, of frequency v and complex-valued amplitude $f(v)$.

$$\Gamma(t) = \int_{-\infty}^{+\infty} f(v)\exp(2\pi jvt)dv \tag{1}$$

where

$$f(v) = \int_{-T}^{+T} \Gamma(t)\exp(-2\pi jvt)dt \tag{2}$$

Note that the limits +/- inf on integral (2) would not always lead to convergence (e.g. an infinitely-persisting noise-like signal), hence +/- T; the distinction is a formality, one takes as large a value of T as is necessary.

#726 - $15.00 US Received January 18, 2002; Revised February 26, 2002

Since $\Gamma(t)$ is real by definition, $f(v)$ is Hermitean: $f(-v) = f^*(v)$, and either of the positive or negative half-domains specifies both the amplitude and the phase of $f(v)$. Due to the Hermitean property, one can dispense with the negative part of the frequency domain and write:

$$\Gamma(t) = 2\,\mathrm{Re}\left[\int_0^{+\infty} f(v)\exp(2\pi jvt)dv\right] \tag{3}$$

If

$$f(v) \equiv a(v)\exp[j\alpha(v)] \tag{4}$$

where $a(v)$ and $\alpha(v)$ modulo (2π) are real functions, the relationship may now be written as

$$\Gamma(t) = 2\int_0^{+\infty} a(v)\cos[2\pi vt + \alpha(v)]dv \tag{5}$$

which is the Fourier cosine integral representation of the interference signal $\Gamma(t)$. Similarly, one can introduce a Fourier sine integral function

$$\Gamma'(t) = 2\int_0^{+\infty} a(v)\sin[2\pi vt + \alpha(v)]dv \tag{6}$$

by changing the phase of each spectral component by a quarter-cycle. $\Gamma'(t)$ is known as the quadrature function of $\Gamma(t)$, and can be obtained by the Hilbert transformation

$$\Gamma'(t) = \frac{1}{\pi} PV\left(\int_{-\infty}^{+\infty} \frac{\Gamma(\tau)}{\tau - t} d\tau\right) \tag{7}$$

where the symbol *PV* means that the principle value in Cauchy's sense of the integral is taken at $t = \tau$. Using Eqs. (4) and (6), one can express the quadrature function $\Gamma'(t)$ in an alternative way

$$\Gamma'(t) = \int_{-\infty}^{+\infty} [-j\,\mathrm{sgn}(v)]f(v)\exp(2\pi jvt)dv \tag{8}$$

Now, the phase-resolved analytic signal associated with the interference signal $\Gamma(t)$ can be defined as

$$\tilde{\Gamma}(t) = A(t)\exp[j\phi(t)] = \Gamma(t) + j\Gamma'(t) \tag{9}$$

It follows that $\tilde{\Gamma}(t)$ can be expressed in the form

$$\tilde{\Gamma}(t) = A(t)\exp[j\phi(t)] = 2\int_0^{+\infty} f(v)\exp(2\pi jvt)dv \tag{10}$$

Eqs. (2) and (10) are what we adopted in our previous phase-resolved OCT/ODT system [6,7,10] for Hilbert transformation. The digital approach to generate analytical signal through Hilbert transformation can be summarized in the following block diagram:

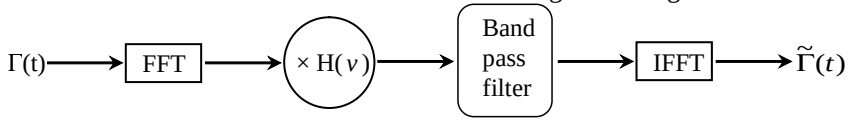

where IFFT is the inverse FFT, and H(v) is the Heaviside function given by:

#726 - $15.00 US
Received January 18, 2002; Revised February 26, 2002

$$H(v)=\begin{cases}0 & v<0\\ 1 & v\geq 0\end{cases} \tag{11}$$

This post-detection digital approach requires a large amount of signal processing, which complicates real-time imaging. Furthermore, the phase-resolved analytic signal $\tilde{\Gamma}(t)$ is a composite of two factors: one that changes rapidly with the frequency of the signal phase factor $\exp[j\phi(t)]$ and a second that changes relatively slowly as a phase-independent amplitude $A(t)$. This is the prerequisite of the analytic signal continuation for reliable implementation of the phase-resolved method. Therefore, phase modulation is required to generate a sufficiently large carrier frequency in the interference signal so that there are at least two fringes per coherence length scanned. Otherwise, phase factor and amplitude can not be properly separated through this post-detection digital signal processing approach.

2.2 Real-time optical approach for phase-resolved OCT/ODT

Real-time optical approach for obtaining the phase-resolved analytic signal is based on the polarization property of light. Essentially, we combine circularly polarized reference and linearly polarized sample signals to produce the interference field that contains the in-phase and quadrature components. We are thus able to detect both components simultaneously based on polarization discrimination and treat them as the real and imaginary parts of the phase-resolved analytic signal. This method for phase information is not restricted to the prerequisite that the phase factor changes much faster than its amplitude.

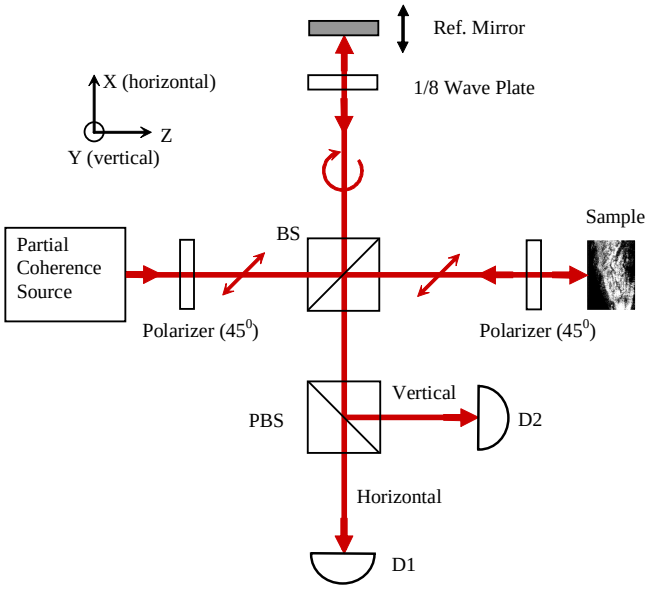

Fig. 1. Schematic diagram of the proposed quadrature interferometer for optical Hilbert transformation. BS: non-polarizing beam splitter, PBS: polarizing beam splitter.

Figure 1 is a schematic diagram of the proposed quadrature interferometer for optical Hilbert transformation. Light emitted from a short coherence source is linearly polarized by a polarizer oriented at a 45 degree angle with respect to the horizontal axis. A non-polarizing beam splitter (BS) splits the input light into reference and sample arms. In the reference arm, a 1/8 wave plate changes linearly polarized light to circularly polarized light. In the sample

#726 - $15.00 US
Received January 18, 2002; Revised February 26, 2002

arm, another polarizer oriented similarly to that in the source port ensures that backscattered light to the interferometer is linearly polarized. The linearly polarized light from the sample and circularly polarized light from the reference are recombined again at the BS and then divided into two orthogonal components by the polarizing beam splitter (PBS).

For convenience, we assume that the horizontal and vertical directions coincide with the x and y axes, and the direction of light propagation is the z-axis. The electric fields for the circularly polarized reference light and the linearly polarized sample light are:

$$\begin{aligned}\vec{E}_s &= (\bar{x}+\bar{y})\int_{t_s} a(t_s)\exp\left[j\phi(t_s)\right]\int_{\nu}\hat{e}(\nu)\exp\left[j2\pi\nu(t-t_s)\right]d\nu dt_s,\\ \vec{E}_r &= (\bar{x}+j\bar{y})R\int_{\nu}\hat{e}(\nu)\exp\left[j2\pi\nu(t-t_r)-j2\pi\nu_C t\right]d\nu.\end{aligned} \tag{12}$$

where $\bar{x}, \bar{y}$ are the unit vectors along the x and y axes, respectively. *a(t)* and *φ(t)* are the reflectance and phase functions of the sample, respectively, t_s is the time delay of the light due to round trip travel from the BS to the reflection site. ν is the frequency of the light source, ν_C is the carrier frequency introduced in the reference arm. The integral with respect to *ν* takes into account the contributions from all spectral components $\hat{e}(\nu)$ of the light source. R is the reflectance of the reference mirror and t_r is the time delay of the light due to the round trip travel from the BS to the reference mirror.

Mixing these fields and determining the intensities of the horizontal and vertical polarization components from a time average square sense, we obtain

$$\begin{aligned}\bar{I}_x &= I_s + I_r + A(t)\cos\left[2\pi\nu_C t+\phi(t)\right],\\ \bar{I}_y &= I_s + I_r + A(t)\sin\left[2\pi\nu_C t+\phi(t)\right].\end{aligned} \tag{13}$$

where

$$I_s = \left\langle\left|\int_{t_s} a(t_s)\exp\left[j\phi(t_s)\right]\int_{\nu}\hat{e}(\nu)\exp\left[j2\pi\nu(t-t_s)\right]d\nu dt_s\right|^2\right\rangle \tag{13a}$$

$$I_r = \left\langle\left|R\int_{\nu}\hat{e}(\nu)\exp\left[j2\pi\nu(t-t_r)-j2\pi\nu_C t\right]d\nu\right|^2\right\rangle \tag{13b}$$

The symbol <…> indicates the time average over the typical detector response time. The amplitude *A(t)* in Eq. (13) can be determined by

$$\begin{aligned}A(t)\exp\left[j\phi(t)\right] &\equiv 2R\int_{t_s} a(t_s)\exp\left[j\phi(t_s)\right]\int_{\nu}\left|\hat{e}(\nu)\right|^2\exp\left[j2\pi\nu(t_r-t_s)\right]d\nu dt_s\\ &= 2R\int_{t_s} a(t_s)\exp\left[j\phi(t_s)\right]G(t_r-t_s)dt_s\\ &= 2Ra(t)\exp\left[j\phi(t)\right]\otimes G(t)\end{aligned} \tag{13c}$$

Here ⊗ is the convolution operation. *G(t)* is the autocorrelation function of the light source which, according to the Wiener Khintchine theorem, is determined by the inverse Fourier transform of the power spectral density. The two terms I_s and I_r in Eq. (13) represent the DC intensity reflected by the sample and reference mirror. In particular, if the DC portions of the measured intensities are removed, we obtain two AC signals I_x, I_y. The two AC signals are then treated as the real and imaginary parts of an analytic signal

$$\tilde{\Gamma}(t) = I_x + jI_y = A(t)\exp\left[j2\pi\nu_C t + j\phi(t)\right] \tag{14}$$

#726 - $15.00 US Received January 18, 2002; Revised February 26, 2002

Except for a phase modulation component, this analytic signal is, in fact, proportional to the convolution of the complex reflectivity of the sample $a(t)\exp[j\phi(t)]$ with the autocorrelation function of the light source *G(t)* as already expressed in Eq. (13c).

Using Eqs. (13) and (14), a phase-resolved analytic signal can be created with less data processing. This is particularly helpful for real-time imaging. Furthermore, as the 90 degree phase shift is directly introduced into the interference signal, this optical approach for Hilbert transformation is not restricted to the prerequisite that the phase factor changes much faster than its amplitude. Therefore, a stable high frequency phase modulator is not necessary, which greatly reduces the system complexity.

3. Methods

The experimental phase-resolved OCT/ODT system for optical Hilbert transformation is illustrated in Fig. 2. The interferometer was constructed on a custom-designed fiber bench with 5 separate fiber-ports connected to the light source, sampling arm, reference arm and two detection channels. The light source is a high-power broadband source centered at 1310 nm with a FWHM spectral bandwidth of 80 nm. The light, after coupling into port A, is linearly polarized by a 45-degree oriented polarizer (P1). A non-polarizing BS then splits the linearly polarized light into the sample and reference arms of the interferometer. In the sample arm, another identical 45-degree oriented polarizer (P2) is inserted next to port B which maintains the backscattered light coming from the sample 45-degree linearly polarized at a PBS. In the reference arm, the combination of a quarter-wave plate (QWP) and linear polarizer (P3) is adopted to assure the reference light is circularly polarized at the PBS. The PBS then separates the two orthogonal interference signals into two channels for detection.

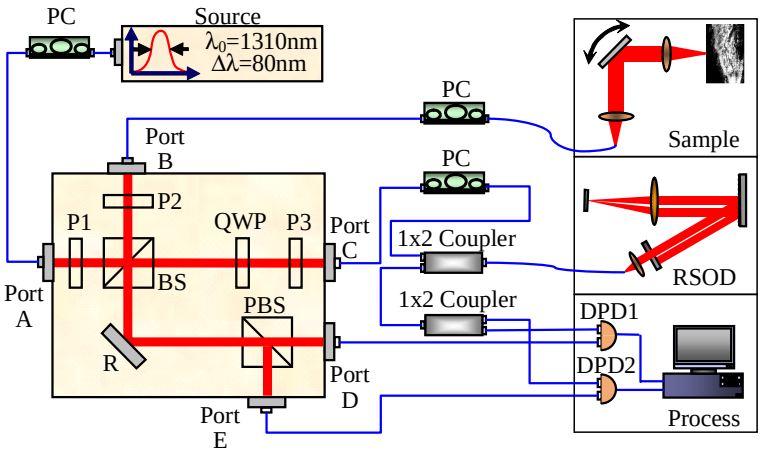

Fig. 2. Experimental phase-resolved OCT/ODT system that implements a quadrature interferometer for optical Hilbert transformation. Ports A-E: pigtailed fiber ports; P1-P3: linear polarizers; QWP: quarter-wave plate; BS: non-polarizing beam splitter; PBS: polarizing beam splitter; RSOD: rapid scanning optical delay line; PC: polarization controller; DPD1 and DPD2: differential photo-detectors with preamplifiers.

A 4 kHz resonant scanner is used in the RSOD for axial scanning. The resonant scanning mirror must be carefully aligned so that no phase modulation will be introduced during axial scanning. Because no phase modulation is introduced in the current OCT/ODT system, the detection bandwidth (2 MHz) and data acquisition rate (5 MHz) is adequate. No significant increase in detection bandwidth and data acquisition rate is required.

#726 - $15.00 US
Received January 18, 2002; Revised February 26, 2002

Two 1x2 50/50 couplers and two differential photo-detectors (DPD1 and DPD2) with preamplifiers are adopted into the system to obtain balanced detection of the signals. Balanced detection removes the low-frequency noise caused by variations in reflection of the RSOD, and reduces the effect of intensity fluctuations from the light source. The system dynamic range is slightly over 80 dB, which is smaller than the system that uses a non-resonant galvanometer. The reduction in dynamic range is primarily due to the higher scanning rate implemented in the current system.

A National Instrument data acquisition card (NI-DAQ) is used in a personal computer to sample the signals in both channels

$$S_x(t) \propto I_x(t) = A(t)\cos\phi(t),$$
$$S_y(t) \propto I_y(t) = A(t)\sin\phi(t). \tag{15}$$

The phase-resolved analytic signal is thus created according to

$$\tilde{\Gamma}(t) = S_x(t) + jS_y(t) = A(t)\exp[j\phi(t)] \tag{16}$$

which allows us to determine both the amplitude and phase information. The computer does not need to perform the digital Hilbert transformation which was the most time-consuming procedure in the previous system [6,7,10]. As a result, the computer can process and display the OCT/ODT images in real-time.

4. Results

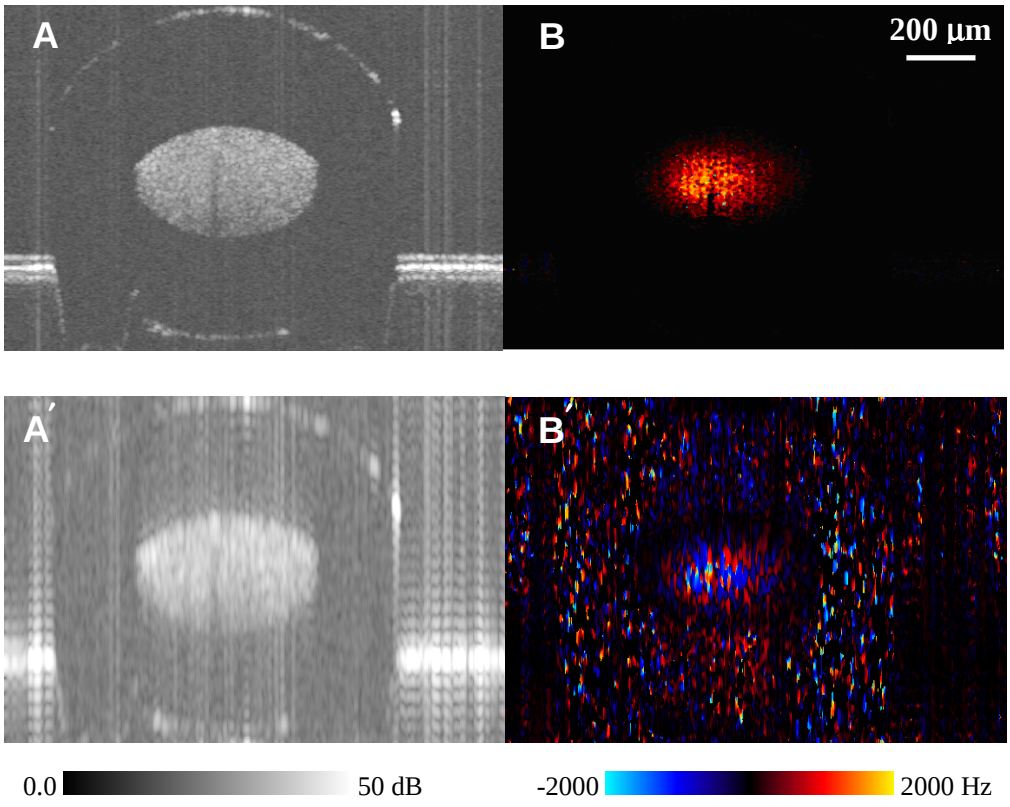

Fig. 3. *In vitro* imaging of the flowing intralipid in a glass conduit. OCT image (A) and ODT image (B) using optical Hilbert transformation; OCT image (A′) and ODT image (B′) using digital Hilbert transformation.

#726 - $15.00 US
Received January 18, 2002; Revised February 26, 2002

To demonstrate feasibility of the current phase-resolved OCT/ODT system without phase modulation using optical Hilbert transformation, an *in vitro* model using a small circular glass conduit (inner diameter of 500 μm) with a flowing suspension of 1% intralipid (μ_s=23cm^{-1}) was investigated. The angle between the probe beam and the direction of flow was approximately 74 degrees. OCT (Fig. 3A) and ODT (Fig. 3B) images were obtained when the suspension of intralipid was infused through the conduit at a velocity of 2 mm/s by a linear syringe pump. In comparison, OCT (Fig. 3A′) and ODT (Fig. 3B′) images using digital Hilbert transformation of the signal $S_x(t)$ from only one channel of the same experimental setup are also shown. Evidently, without the required phase modulation to generate an appropriate carrier frequency in the interference signal, the approach based on digital Hilbert transformation is not reliable enough to obtain the phase and amplitude information correctly. The geometrical distortion of the circular glass conduit in OCT images is mainly due to the refractive index difference between glass and air. Nonlinear axial scanning produced by the sinusoidal oscillations of the resonant scanner further contributes to this distortion.

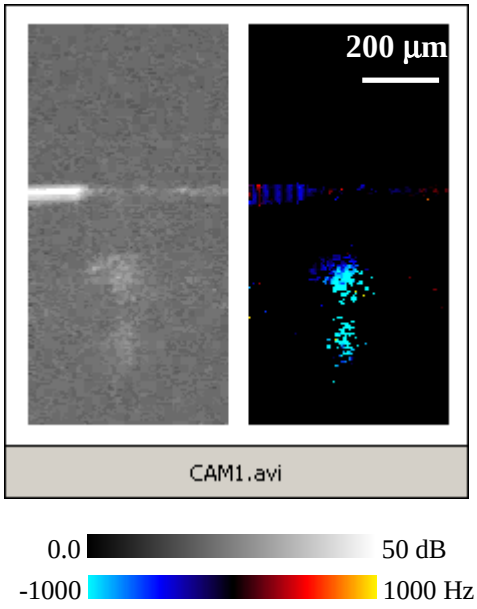

Fig. 4. Recordings (1.04 MB) of real-time *in vivo* OCT/ODT images (100 x50 pixels) of two veins in the CAM.

To demonstrate the capability of the current phase-resolved OCT/ODT system using optical Hilbert transformation for real-time imaging, the *in vivo* chick chorioallantoic membrane (CAM) model was investigated. The CAM is a well-established model for studying microvasculature and has been used extensively in our laboratory to investigate the effects of vasoactive drugs as well as laser irradiation on blood vessels [2]. After removing the apex of the chick egg shell, we non-invasively imaged the CAM microvasculature within a transparent matrix. A minimum of 4 repeat-time of the sequential scanning at each lateral pixel position is required to reconstruct the ODT image reliably. Accordingly, the frame rate for OCT/ODT images with 200 axial scans can be acquired at 20 frames per second in the current phase-resolved OCT/ODT system using optical Hilbert transformation. However, because the highest frame rate of our video capture is limited to 15 frames per second, we have to reduce the actual frame rate of the OCT/ODT images by increasing the repeat-time to 16. The benefit of this increased repeat-time is an improved signal to noise ratio in the ODT

#726 - $15.00 US
Received January 18, 2002; Revised February 26, 2002

image. Figure 4 demonstrates the real-time *in vivo* OCT/ODT images of blood flow in the CAM with 800 axial scans. Two veins under the CAM membrane are evident in both OCT and ODT images. Figure 5 shows another real-time *in vivo* OCT/ODT images of blood flow in the CAM consisting of one vein and one artery. Both structure and blood flow velocity images with 1280 axial scans are acquired. The pulsation nature of the artery can be clearly observed.

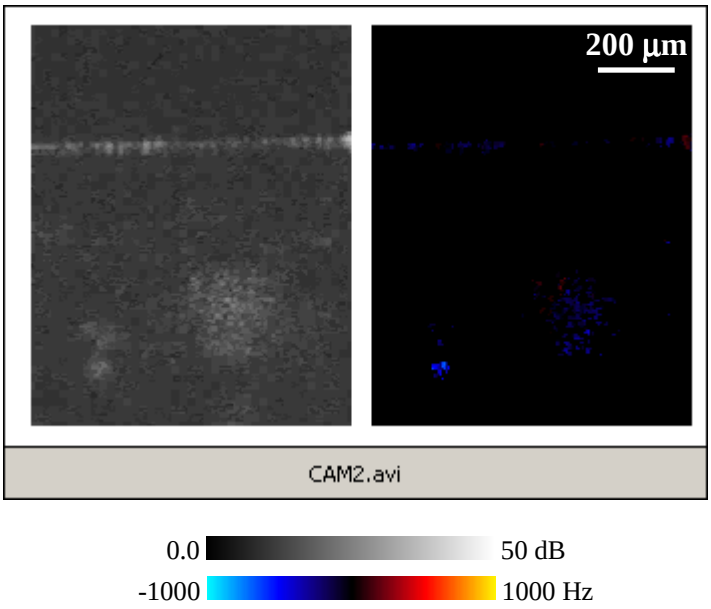

Fig. 5. Recordings (726 KB) of real-time *in vivo* OCT/ODT images (100 x80 pixels) of one vein and one artery in the CAM.

5. Conclusions

We have developed a novel real-time phase-resolved OCT/ODT system using optical Hilbert transformation. A stable high frequency phase modulator is not necessary in this technique, which greatly reduces the requirements for the detection bandwidth of the photo-detector and simplifies data acquisition and signal processing. This technique might be very useful in the clinical management of patients where real-time monitoring of blood flow changes is essential.

Acknowledgements

We acknowledge the valuable contributions from Leaky Liaw and Jianjun Miao. This work was supported by research grants awarded from the National Institutes of Health (HL-64218, EB-00293, RR-01192 and GM-58785), National Science Foundation (BES-86924), and DARPA BioFlips Program (N66001-C-8014). Institutional support from the Air Force Office of Scientific Research (F49620-00-1-0371) and Beckman Laser Institute Endowment are also gratefully acknowledged. Please address all correspondence to Z. Chen at zchen@bli.uci.edu.